Pharm Res (2014) 31:1665–1675
DOI 10.1007/s11095-013-1271-5

RESEARCH PAPER

A Novel Formulation Based on 2,3-Di(tetradecyloxy) propan-1-amine Cationic Lipid Combined with Polysorbate 80 for Efficient Gene Delivery to the Retina

Gustavo Puras Ochoa • Jon Zárate Sesma • Mireia Agirre Díez • Ariadna Díaz-Tahoces • Marcelino Avilés-Trigeros • Santiago Grijalvo • Ramón Eritja • Eduardo Fernández • Jose Luis Pedraz

Received: 29 July 2013 / Accepted: 19 December 2013 / Published online: 22 January 2014

ABSTRACT

Purpose The aim of the present study was to evaluate the potential application of a novel formulation based on a synthesized cationic lipid 2,3-di(tetradecyloxy)propan-1-amine, combined with polysorbate 80 to deliver the pCMS-EGFP plasmid into the rat retina.

Methods We elaborated lipoplexes by mixing the formulation containing the cationic lipid and the polysorbate 80 with the plasmid at different cationic lipid/DNA ratios (w/w). Resulted lipoplexes were characterized in terms of size, charge, and capacity to condense, protect and release the DNA. *In vitro* transfection studies were performed in HEK-293 and ARPE-19 cells. Formulations were also tested *in vivo* by monitoring the expression of the EGFP after intravitreal and subretinal injections in rat eyes.

Results At 2/1 cationic lipid/DNA mass ratio, the resulted lipoplexes had 200 nm of hydrodynamic diameter; were positive charged, spherical, protected DNA against enzymatic digestion and transfected efficiently HEK-293 and ARPE-19 cultured cells exhibiting lower cytotoxicity than LipofectamineTM 2000. Subretinal administrations transfected mainly photoreceptors and retinal pigment epithelial cells; whereas intravitreal injections produced a more uniform distribution of transfection through the inner part of the retina.

Conclusions These results hold great expectations for other gene delivery formulations based on this cationic lipid for retinal gene therapy purposes.

Electronic supplementary material The online version of this article (doi:10.1007/s11095-013-1271-5) contains supplementary material, which is available to authorized users.

G. P. Ochoa • J. Z. Sesma • M. A. Díez • A. Díaz-Tahoces • M. Avilés-Trigeros • S. Grijalvo • R. Eritja • E. Fernández • J. L. Pedraz (✉)
University of the Basque Country, Vitoria, Spain
e-mail: joseluis.pedraz@ehu.es

KEY WORDS cationic lipids · gene therapy · lipoplexes · non-viral vectors · retina

INTRODUCTION

Many currently incurable blinding disorders in the developed world affecting the retina such as glaucoma, retinitis pigmentosa, or age-related macular degeneration have a well-known genetic background localized on retinal ganglion cells, photoreceptors or retinal pigment epithelium (1). Therefore, research on retinal gene therapy offers hope and represents a logical and promising approach to develop gene based treatments (2), although it is still far to be considered as a mainstream medicine option, mainly because new safe and effective vectors need to be developed (3).

Generally, the eye is an attractive target for gene therapy due to its relative small size, immune-privileged characteristics and easy accessibility. Furthermore, the eye benefits from a well-defined anatomy and a low diffusion into systemic circulation, minimizing the potential adverse reactions that may follow after intraocular injection of foreign antigens (4,5). Furthermore, as the media is transparent, the gene transfer process can be easily tracked through non invasive techniques and minor changes of visual function can be monitored by sensitive methods (3).

At present, most gene delivery systems to the retina use viral and non-viral vectors (5,6). Among viral vectors, the most commonly used are the adeno-associated viruses (AAV). First encouraging clinical trials in patients suffering from Leber's congential amaurosis were published in 2008 (7–9). Nowadays, new safer recombinant AAV serotypes have been used to get long term and selective transgene expression into different retinal cells (10,11); however, justifiable concerns have been raised over the risk of oncogenesis, immunogenicity

and inflammatory responses (12,13). In addition, the limited size of the gene that may be transfected, the high production costs of preparative procedures and the classification of non-viral methods as drugs rather than as biologics by the regulatory authorities have garnered the interest to invest on new non-viral gene transfer methods (2,14). Among non-viral vectors, the most common chemical method of delivering plasmids to the retina involves the formation of cationic lipid-DNA complexes (lipoplexes) (15–17). However, concerns related to effectiveness and toxicity has motivated the scientific community in the past decade to invest on new lipoplexes formulations in order to improve transfection efficiency and decrease cytotoxicity (18), which may yield an efficacious method of gene delivery to the retina in the future.

Recently, it has been reported the synthesis and *in vitro* evaluation of novel lipid-oligonucleotide conjugates based on the cationic lipid 2,3di(tetradecyloxy)propan-1-amine for RNA interference studies (19). In light of these promising results, we elaborated a novel formulation based on the aforementioned cationic lipid 2,3-di(tetradecyloxy)propan-1amine combined with polysorbate 80 as emulsifier to form lipoplexes. pCMS-EGFP was employed as reporter plasmid. Resulted lipoplexes were characterized at different cationic lipid/DNA mass ratios (w/w) by transmission electron microscopy (TEM) and by their ability to complex and protect the DNA from deoxyribonuclease I (DNase I) enzymatic digestion. Surface charge density and size diameter of lipoplexes were measured, and the most promising formulations were selected for *in vitro* transfection studies in human embryonic kidney cell line (HEK-293), and in the human retinal epithelium pigment cell line (ARPE-19). *In vivo* experiments were performed to evaluate the efficiency of the novel formulation to deliver DNA into retinal cells. We administered the lipoplexes by subretinal and intravitreal injections. Expression of the enhanced green fluorescent protein (EGFP) was evaluated by confocal microscopy at 72 h in different cells and layers of the retina.

MATERIALS AND METHODS

Materials

Commercially available reagents and solvents were of reagent grade and used without further purification. TLC was performed on silica gel sheets (Alugram Sil G/UV). All compounds were characterized by ^{1}H-NMR at room temperature and were performed in $CDCl_3$ and recorded on a Mercury 400 MHz spectrometer (Unitat de RMN, Serveis Científico-Técnics, Universitat de Barcelona). Chemical shifts are reported as δ values using TMS as internal standard for proton spectra and relative to the residue solvent peak. HEK-293 cells, ARPE-19 cells, Eagle's Minimal Essential medium with Earle's BSS and 2 mM l-glutamine (EMEM) were obtained from the American Type Culture Collection (ATCC). Dulbecco's Modified Eagle's medium Han's Nutrient Mixture F-12 (1:1) was purchased from GIBCO (San Diego, California, US). The plasmid pCMS-EGFP, was purchased from PlasmidFactory (Bielefeld, Germany). The gel electrophoresis materials and ethidium bromide solution were acquired from Bio-Rad (Madrid, Spain). DNase I, sodium dodecyl sulphate (SDS), Hoechst 33342 dye and PBS, were purchased from Sigma–Aldrich (Madrid, Spain). Opti-MEM®I reduced medium, antibiotic/antimicotic solution and Lipofectamine™ 2000 were acquired from Invitrogen (San Diego, California, US). Polysorbate 80 (Tween 80) was provided by Vencaser (Bilbao, Spain). The BD Viaprobe kit was provided by BD Biosciences (Belgium). Adult Sprague–Dawley rats were purchased from Harlan Laboratories (Barcelona, Spain).

Synthesis of the Lipid

2,3-di(tetradecyloxy)propan-1-amin cationic lipid was synthesized by modifying slightly the experimental protocol described previously (20), using a biphasic system consisting of toluene and an aqueous sodium hydroxide mixture in the presence of Bu_4NHSO_4 along with the appropiate 1-bromotetradecane (see Supplementary Material). After removing the Boc group under acid conditions (10% of trifluoroacetic acid in dichloromethane), the expected free amine in its trifluoroacetate salt was successfully captured by using Amberlite® IRA-900 $NaCO3^-$ form (see Supplementary Material). All ^{1}H-NMR spectra were consistent with those reported in the literature.

Preparation of the Lipoplexes

Resulted cationic lipid was dispersed in an Opti-MEM® I solution containing the emulsifier polysorbate 80 at 0.1% (w/v) to get a final cationic lipid concentration of 0.5 mg/ml. The emulsion was then vortexed for 1 min and briefly sonicated at 37°C until became clear and transparent. To get the lipoplexes at different cationic lipid/DNA ratios (w/w), an appropriate volume of a pCMS-EGFP plasmid 0.5 mg/ml stock solution in Opti-MEM® was added under gentle vortexing for 20s. Lipoplexes were incubated for 30 min at room temperature before use to enhance electrostatic interactions.

Characterization of Lipoplexes

The hydrodynamic diameter and superficial charge of the lipoplexes at different cationic lipid/DNA ratios (w/w) were determined on a Zetasizer Nano ZS (Malvern Instruments, UK) by dynamic light scattering (DLS) and laser doppler

velocimetry (LDV), respectively. All measurements were carried out in triplicate. Lipoplexes were diluted in NaCl 0.1 mM Milli-Q water before measuring size and zeta potential.

Morphology of lipoplexes was visualized using TEM analysis. Briefly, 5 µl of the samples were adhered onto glow discharged carbon coated grids for 60 s. Remaining liquid was removed by blotting on paper filter and stained with 2% uranyl acetate for 60 s at pH 6.0 to enhance the contrast. Samples were visualized under the microscope, TECNAI G2 20 TWIN (FEI, Eindhoven, The Netherlands), operating at an accelerating voltage of 200 KeV in a bright-field image mode. Digital images were acquired with an Olympus SIS Morada digital camera.

Binding, DNase I Protection and SDS-Induced Release of DNA

Naked DNA or lipoplexes samples (20 µl) containing different cationic lipid/DNA ratios (w/w) at a constant amount of DNA (200 ng of the plasmid per well) were subjected to electrophoresis on an ethidium bromide-containing agarose gel (0.8%). The gel was immersed in a tris-acetate-EDTA buffer and exposed for 30 min to 120 V. Bands were observed with a model TFX-20 M transilluminator (Vilber-Lourmat, Germany), and the images were captured using a digital camera from BioRad, DigiDoc model. To analyze the release of DNA from the formulation, 20 µl of a 2% SDS solution was added to the samples. Protection capacity of the lipoplexes against enzymatic digestion was studied after adding DNase I (final concentration 1 U DNase I/2.5 µg DNA). Afterwards, the mixtures were incubated at 37°C for 30 min. Finally, 2% SDS solution was added to release DNA from lipoplexes. The integrity of the DNA in each sample was compared with untreated DNA.

In Vitro Transfection Experiments

HEK-293 and ARPE-19 cells were seeded in 24-well plates at an initial density of 15×10^4 and 10×10^4 cells/well, with 1 ml EMEM containing 10% horse serum and with 1 ml D-MEM/F-12 containing 10% fetal bovine serum, respectively. Then, at a confluence level of 70–80%, the media was removed and cells were exposed to different cationic lipid/DNA ratio (w/w) lipoplexes (1.25 µg DNA) diluted in serum-free Opti-MEM® I solution for 4 h at 37°C. Following the incubation time, the medium was refreshed with 1 ml of complete medium and cells were allowed to grow for further 72 h until fluorescent microscopy and flow cytometry analysis. Experiments with Lipofectamine™ 2000 were prepared following the manufacturer's protocol.

Qualitative expression of EGFP was examined using an inverted microscope with simultaneous epi-fluorescence and phase contrast observation (Eclipse TE200-S, Nikon Instruments Europe B.V., Amstelveen, The Netherlands). Quantitative expression of the reported gene was determined on a FACSCalibur system flow cytometer (Becton Dickinson Biosciences, San Jose, USA). Cells were washed in PBS and detached with 300 µl of 0.05% trypsin/EDTA. Then, cells were centrifuged and the supernatant was discarded. Before flow cytometry analysis, the pellet was resuspended in PBS and diluted in FACSFlow (1:1). Transfection efficiency was analyzed at 525 nm (FL_1). 5 µL of he BD-Via Probe reagent, 7-Amino-actinomycin D (7-AAD) were added to each sample for cell viability determinations. BD-Via Probe positive cells were excluded from the EGFP expression analysis. The fluorescence corresponding to dead cells was measured at 650 nm (FL_3). Control samples (non-transfected cells) were displayed on a forward scatter (FSC) *versus* side scatter (SSC) dot plot to establish a collection gate and exclude cells debris. Other control samples containing Lipofectamine™ 2000 transfected cells without BD-Via Probe, and non-transfected cells with BD-Via Probe were used to compensate FL_2 signal in FL_1 and FL_3 channels. For each sample 10,000 events were collected.

In Vivo Transfection Experiments

Adult male Sprague Dawley rats (6–7 weeks old, 150–200 g weight) were used as experimental animals. All experimental procedures were carried out in accordance with the Spanish and European Union regulations for the use of animals in research and the Association for Research in Vision and Ophthalmology (ARVO) statement for the use of animals in ophthalmic and vision research and supervised by the Miguel Hernandez University Standing Committee for Animal Use in Laboratory. All the experimental manipulations were carried under general anaesthesia induced with an intraperitoneal (i.p) injection of a mixture of ketamine (70 mg/kg, Ketolar®, Parke–Davies, S.L., Barcelona, Spain) and xylazine (10 mg/kg, Rompún®, Bayer, S.A., Barcelona, Spain). For recovery from anaesthesia, an ointment containing tobramycin (Tobrex® pomada oftálmica, Alcon S.A., Barcelona, Spain) was applied on the cornea. Animals were sacrificed by an i.p injection of an overdose of 20% sodium pentobarbital (Dolethal Vetoquinol®, Especialidades Veterinarias, S.A., Alcobendas, Madrid, Spain).

Intravitreal and Subretinal Administration

Animals were randomly divided into six groups ($n=4$ each) and each one received either by intravitreal or by subretinal route a solution (5 µl of 10 mM HEPES, pH 7.1) of naked plasmid (100 ng) or a suspension based on lipoplexes at 2/1 or 4/1 cationic lipid/DNA ratios containing 100 ng of the plasmid. Injections were performed under an operating microscope (Zeiss OPMI® pico; Carl Zeiss Meditec GmbH, Jena, Germany) with the aid of a Hamilton microsyringe (Hamilton

Co., Reno, NV). A bent 34-gauge needle was used to inject into the vitreous of the left eye, immediately adjacent to the ora serrata without touching the lens. To deliver the lipoplexes into the subretinal space the needle was passed through the sclerotomy 2 mm posterior to ora serrata and in a tangential direction toward the posterior retinal pole along the subretinal space. Successful administration was confirmed by the appearance of a partial retinal detachment by direct ophthalmoscopy of the eye fundus. The untreated right eye, served as a control. Seventy two hours post-injection, the rats from each experimental group (DNA treated group, and groups treated with lipoplexes at 2/1 and 4/1 ratios) were sacrificed and perfused with 0.9% saline followed by 4% paraformaldehyde in 0.1 M phosphate buffer (pH 7.2–7.4) at 4°C.

Evaluation of EGFP Expression in Rat Retinas

For whole-mount preparations, both eyes from two rats of each group were enucleated and immersed for 1 h in a solution of 4% paraformaldehyde in PBS. Later, the retinas were dissected as wholemounts by making four radial cuts. Retinal orientation was maintained by making the deepest radial cut in the superior retina. The retinas were postfixed for 1 h in the same fixative, rinsed in PBS, and mounted vitreal side up on poly-L-lysine coated microscope slides, covered with anti-fading mounting media containing 50% glycerol and 0.04% *p*-phenylenediamine in 0.1 M sodium carbonate buffer (pH 9.0). For sagittal section preparations, both eyes from two rats of each group were enucleated, and the anterior segments, including the lens, were removed. Posterior eyecups were fixed for 1 h with 4% paraformaldehyde in 0.1 M PBS, followed by several washes in PBS. Samples were then immersed in 30% sucrose in PBS overnight at 4°C for cryoprotection. Eyecups were embedded and oriented in optimal cutting temperature (O.C.T.™) compound (Tissue-Tek®; Sakura Finetek Europe B.V., Alphen and den Rijn, The Netherlands) and frozen in 2-methylbutane cooled in liquid nitrogen at −60°C. Radial sections (15 μm) were cut with a cryostat (HM 550; Microm International GmbH, Walldorf, Germany), mounted on SuperFrost® Plus microscope slides (VWR International bvba, Leuven, Belgium). To counterstain all retinal nuclei, sections were stained with 5 μg/ml Hoechst 33342 dye for 5 min and then thoroughly washed with PBS 0.1 M and covered with anti-fading mounting media.

EGFP expression and Hoechst 33342 staining were evaluated with a Leica TCS SPE spectral confocal microscope (Leica Microsystems GmbH, Wetzlar, Germany). Images were processed, montaged and composed digitally using ImageJ, (National Institutes of Health, Bethesda, MD) and Adobe® Photoshop® CS5.1 (Adobe Systems Inc, San Jose, CA) software. Hoeschst 33342 staining was pseudocolored in red for better contrast.

Statistical Analysis

Statistical analysis was completed using the InStat programme (GraphPad Software, San Diego, CA, USA). Differences between groups at significance levels of 95% were calculated by the Student's *t* test. In all cases, *P* values <0.05 were regarded as significant. Normal distribution of samples was assessed by the Kolmogorov-Smirnov test, and the homogeneity of the variance by the Levene test. Data were presented as mean ± SD, unless stated otherwise.

RESULTS

Lipoplexes Characterization

The average size and zeta potential at different cationic lipid/DNA ratios (w/w) is illustrated in Fig. 1a. Particle size clearly increased gradually with the ratio from 149 nm (0.5/1) to a maximum of 260 nm (4/1). At this point, particle size decreased as the ratio increased, reaching 195 nm at 8/1 ratio. In all cases, polydispersity index was below 0.3 (data not shown). Regarding zeta potential, negative values were obtained at 0.5/1 and 1/1 ratios (−33 and −16 mV respectively). First positive zeta potential value 7.3 mV, was reached at 2/1 ratio, and thereafter increased until a maximum of 13.2 mV at 6/1 ratio.

The morphology and size of lipoplexes at 2/1 ratio were assessed by TEM as illustrated in Fig. 1b and c (original magnification 50.000× and 80.000× respectively). Spherical lipoplexes of approximately 200 nm were observed under our experimental conditions.

Binding, DNase I Protection, and SDS-induced Release of DNA

Figure 2 shows the results obtained in the agarose gel electrophoresis assay. No band corresponding to free DNA was observed on lanes 7, 10 and 13, which means that all DNA was bound to the formulation at 4/1, 6/1 and 8/1 ratios. At 2/1 ratio, practically all the DNA was bound to the formulation (lane 4). Regarding the SDS-induced release, all the DNA was released at 2/1 ratio (lane 5), however at higher ratios (4/1, 6/1 and 8/1) a small amount of DNA remained bound to the formulations (lanes 8, 11 and 14 respectively). The presence of supercoiled (SC) bands on lanes 6, 9, 12 and 15 reveals that lipoplexes prepared at all ratios protected the DNA against enzymatic digestion; however only at 2/1 ratio (lane 6) all the DNA was released from the formulation. Lane 1, 2 and 3 correspond to untreated DNA, DNA treated with 2% SDS and DNA incubated with DNase I and thereafter treated with 2% SDS respectively. The absence of signal in

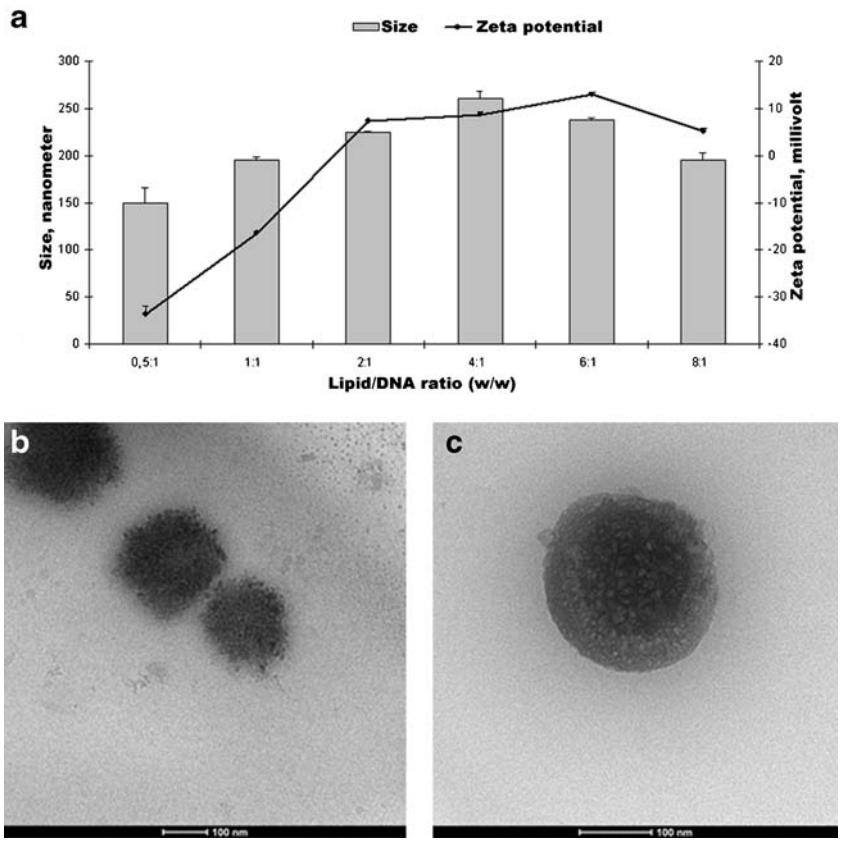

Fig. 1 Lipoplexes characterization. (**a**) Effect of cationic lipid/DNA ratio (w/w) on size and zeta potential (mean ± SD, $n = 3$). (**b**) TEM micrograph of lipoplexes at 2/1 charge ratio, original magnification 50.000×. (**c**) TEM micrograph of lipoplexes at 2/1 charge ratio, original magnification 80.000×.

lane 3 suggests that the enzyme worked properly in our experimental conditions.

In Vitro Transfection Studies

Pictures on Fig. 3 show that the number of transfected cells increased gradually with the mass ratio, both in HEK-293 (Fig. $3A_2$, B_2 and C_2) and in ARPE-19 cells (Fig. $3E_2$, F_2 and G_2). However, the highest values were obtained with Lipofectamine™ 2000 (Fig. $3D_2$ and H_2). Cells examined under phase contrast microscopy revealed a healthy morphology on HEK-293 when treated with lipoplexes (Fig. $3A_1$, B_1 and C1). However, Lipofectamine™ 2000 treatment changed the morphology of the cells (Fig. $3D_1$). Regarding ARPE-19 cells, changes in the morphology of the cells were evident when cells were exposed to Lipofectamine™ 2000 (Fig. $3H_1$). At 2/1 and 4/1 mass ratios, ARPE-19 cells were healthy under the phase contrast microscopy examination (Fig. $3E_1$ and F_1).

Transfection efficiency and cell viability was quantified by flow cytometry (Fig. 4). Figure 4a confirmed the data obtained by microscopy, as the percentage of transfected cells increased gradually to the mass ratio, both in HEK-293 (white bars) and in ARPE-19 cells (black bars). At all ratios tested, the percentage of transfection was slightly higher in HEK-293 cells, which ranged from 34% at 2/1 ratio to 78% at 6/1 ratio (data normalized to Lipofectamine™ 2000; absolute values were 15.3% and 35.1% respectively). The percentage of transfection in ARPE-19 cells ranged from 30% at 2/1 ratio to 71% at 6/1 ratio (data normalized to Lipofectamine™ 2000; absolute values were 12% and 28.4% respectively). To further relate

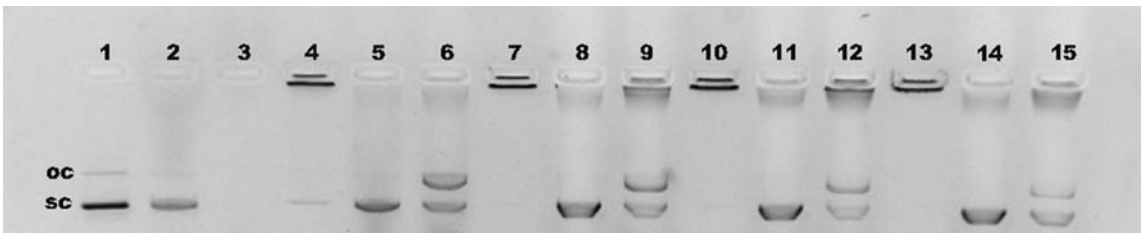

Fig. 2 Binding, protection, and SDS-induced release of DNA visualized by agarose electrophoresis. *Lanes 1–3* correspond to free DNA; *lanes 4–6*, cationic lipid/DNA 2/1; *lanes 7–9*, cationic lipid/DNA 4/1; *lanes 10–12*, cationic lipid/DNA 6/1; *lanes 13–15*, cationic lipid/DNA 8/1. Lipoplexes were treated with SDS (*lanes 2, 5, 8, 11* and *14*) and DNase I + SDS (*lanes 3, 6, 9*, and *15*). OC: open circular form, SC: supercoiled form.

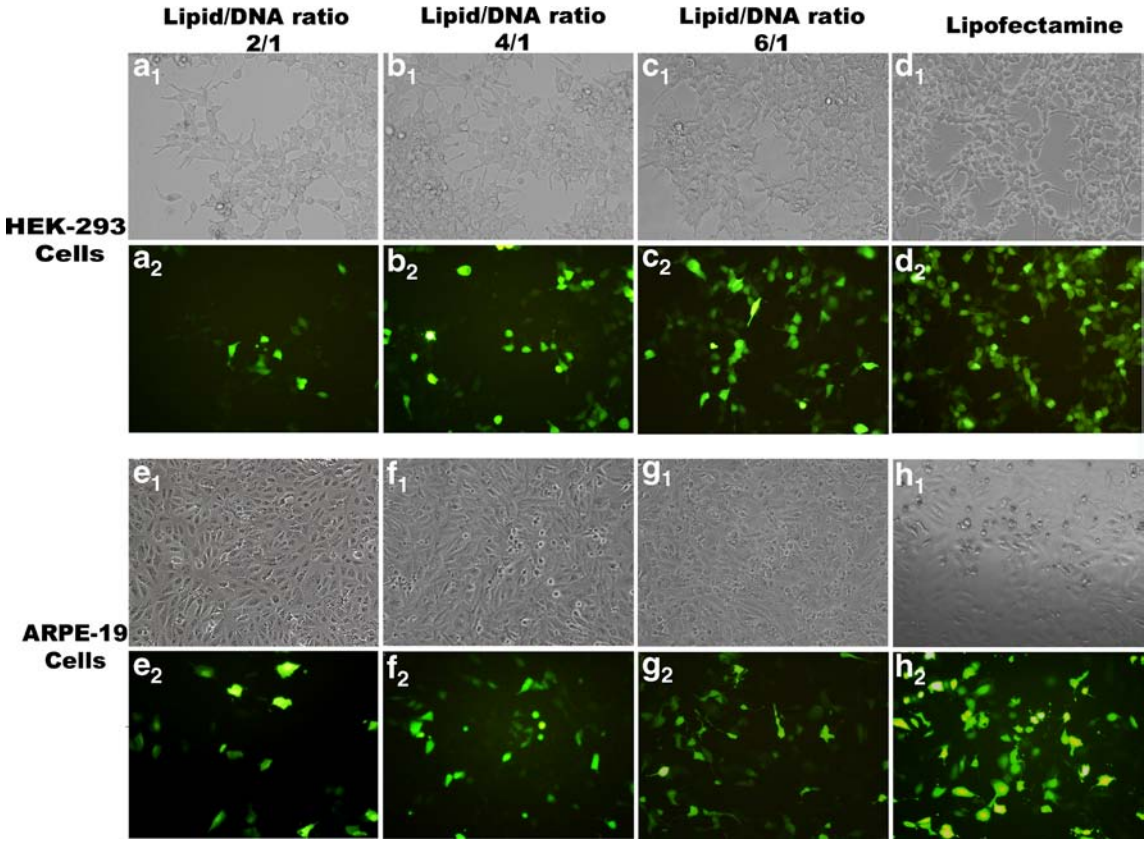

Fig. 3 Phase contrast and fluorescent micrographs of HEK-293 (A_1-D_2) and ARPE-19 cells (E_1-H_2) transfected with lipoplexes at different ratios and Lipofectamine™ 2000. Images were acquired at 72 h post-transfection, original magnification 20×.

the percentage of transfected cells and the level of protein expression, we measured the mean fluorescent intensity (MFI) of transfected cells (Fig. 4b, bars). In HEK-293, MFI increased proportionally to the mass ratio, and for all formulations tested was significantly higher than Lipofectamine™ 2000. However, in ARPE-19, MFI at 2/1 and 4/1 ratios was similar, and clearly decreased at 6/1 ratio to a level inferior to Lipofectamine™ 2000. Regarding cell viability, Lipofectamine™ 2000 was significantly more toxic to HEK-293 (75% viability) and ARPE-19 (71% viability) cells than the lipoplexes at all ratios tested (Fig. 4b, lines). In ARPE-19 cells, viability clearly decreased from 97% at 2/1 and 4/1 mass ratios to 85% at 6/1 ratio, however, in HEK-293 cells viability was around 85% for all ratios examined.

Figure 4c and d represent the flow cytometry dot-plots (FSC-SSC and FL_1-FL_3) and the histograms (FL_1) of an individual measurement for HEK-293 and ARPE-19 cells respectively.

In Vivo Transfection Experiments

EGFP expression was detected only in the group treated with lipoplexes at 2/1 ratio for both subretinal and intravitreal administrations (Figs. 5 and 6). No gene expression was detected after administration of the DNA solution, and little to no-transfection was observed with the lipoplexes at 4/1 ratio (data not shown). The level of protein expression strongly varied depending on the location of the injection. Thus, after subretinal injection (Fig. 5), protein expression was found mainly in the retinal pigment epithelium (RPE) and photoreceptor outer segments (Fig. 5b), although it was also expression in the outer nuclear layer (ONL) and in several cells located at the inner nuclear layer (INL) (Fig. 5c). After intravitreal injection (Fig. 6), transfected cells were more uniformly distributed mainly in the ganglion cell layer (GCL) and inner nuclear layer (INL) (Fig. 6b, c, d). Evidence of toxicity was not detected, irrespective of the formulation administered.

Fig. 4 Flow cytometry data of HEK-293 and ARPE-19 cells. (**a**) Percentage of transfected cells with lipoplexes at different ratios. Data were normalized to Lipofectamine™ 2000 (mean ± SD; n = 3). (**b**) Mean fluorescent intensity, MFI ($^{\#}P < 0.05$ relative to Lipofectamine™ 2000) and viability ($^{*}P < 0.05$ relative to Lipofectamine™ 2000) of cells transfected with different formulations (mean ± SD; n = 3). (**c**) Flow cytometry dot-plots (FSC-SSC and FL_1-FL_3) and histograms (FL_1) of HEK-293 cells transfected with lipoplexes at different ratios and Lipofectamine™ 2000. (**d**) Flow cytometry dot-plots (FSC-SSC and FL_1-FL_3) and histograms (FL_1) of ARPE-19 cells transfected with lipoplexes at different ratios and Lipofectamine™ 2000. FL_1 channel corresponds to EGFP and FL_3 channel to 7-AAD.

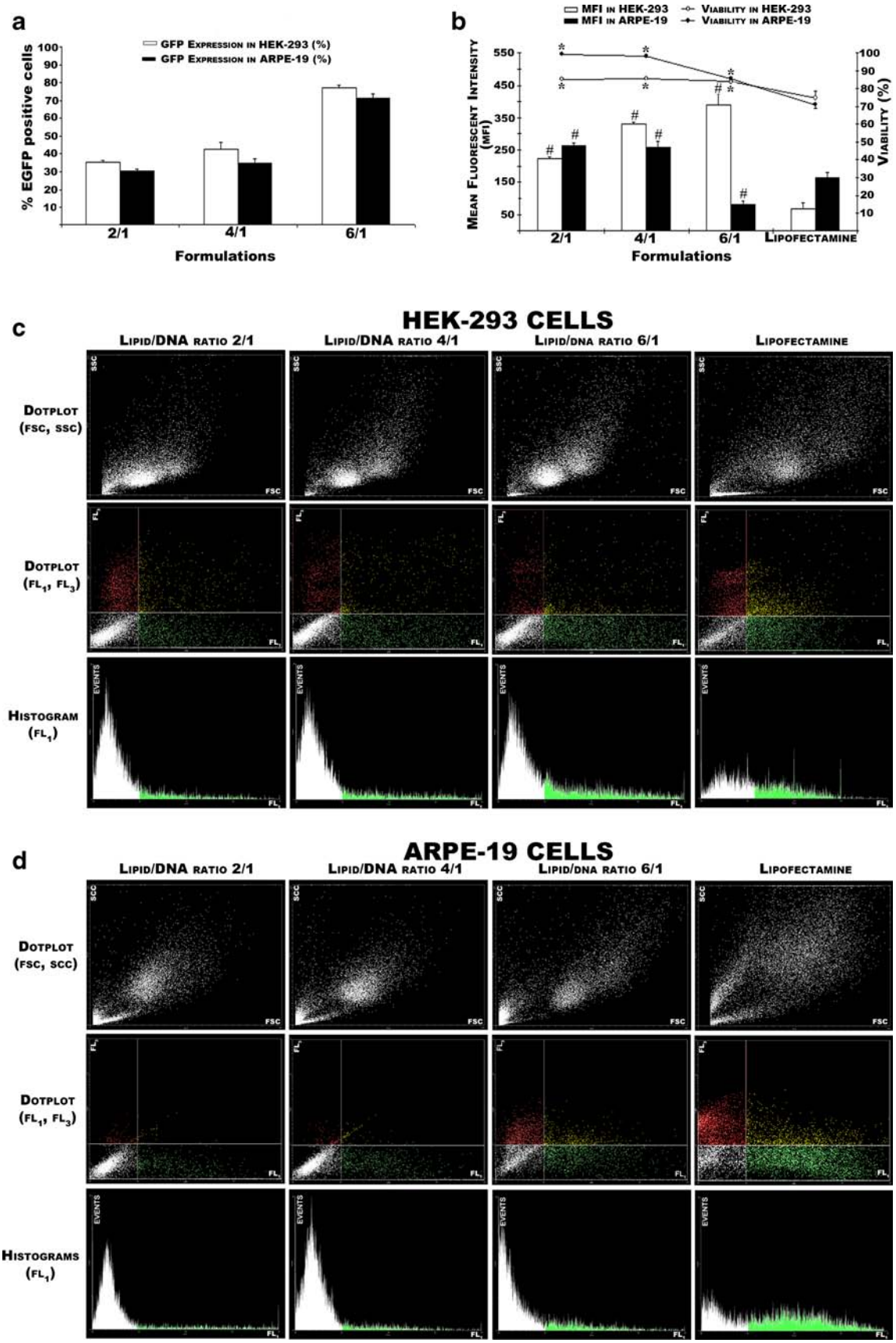
a
GFP Expression in HEK-293 (%)
GFP Expression in ARPE-19 (%)
% EGFP positive cells
2/1
4/1
6/1
Formulations
b
MFI in HEK-293
MFI in ARPE-19
Viability in HEK-293
Viability in ARPE-19
Mean Fluorescent Intensity (MFI)
Viability (%)
2/1
4/1
6/1
Lipofectamine
Formulations
c
HEK-293 CELLS
Lipid/DNA ratio 2/1
Lipid/DNA ratio 4/1
Lipid/DNA ratio 6/1
Lipofectamine
Dotplot (FSC, SSC)
Dotplot (FL1, FL3)
Histogram (FL1)
d
ARPE-19 CELLS
Lipid/DNA ratio 2/1
Lipid/DNA ratio 4/1
Lipid/DNA ratio 6/1
Lipofectamine
Dotplot (FSC, SCC)
Dotplot (FL1, FL3)
Histograms (FL1)

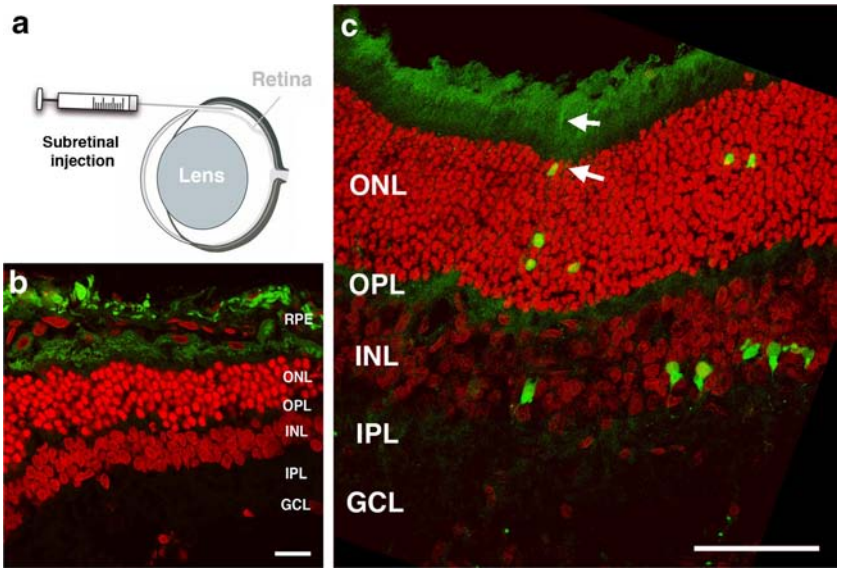

Fig. 5 *In vivo* gene expression of EGFP after administration of lipoplexes at 2/1 ratio to rats 72 h post subretinal injection. (**a**) Schematic drawing of the subretinal injection. (**b**) Confocal fluorescence microscopy image of a 15-μm retina cross-section close to the place of the injection, showing the different layers of the retina. Note the presence of EGFP expression (*green* labelling) in the RPE and choroid. (**c**) Cellular EGFP expression is presented in the ONL, showing some photoreceptor near-completely labelled (*arrows*), and in the INL. Cell nuclei were counterstaining with Hoechst 33342 (pseudocolored *red*). RPE (Retinal Pigment Epithelium layer), ONL (Outer nuclear layer), OPL (Outer plexiform layer), INL (Inner nuclear layer), IPL (Inner plexiform layer), GCL (Ganglion cell layer). Scale bar = 40 μm.

DISCUSSION

Despite viral vectors have been widely used for retinal gene therapy purposes (6,21) important safety concerns have hindered further development and their potential applications for human gene therapy. Therefore, research on non-viral vectors has gained *momentum*, and represents a promising alternative approach to deliver genetic material into the retina; however, additional work, including the synthesis of new safer and effective vectors, is required to yield an efficacious method of gene delivery (2).

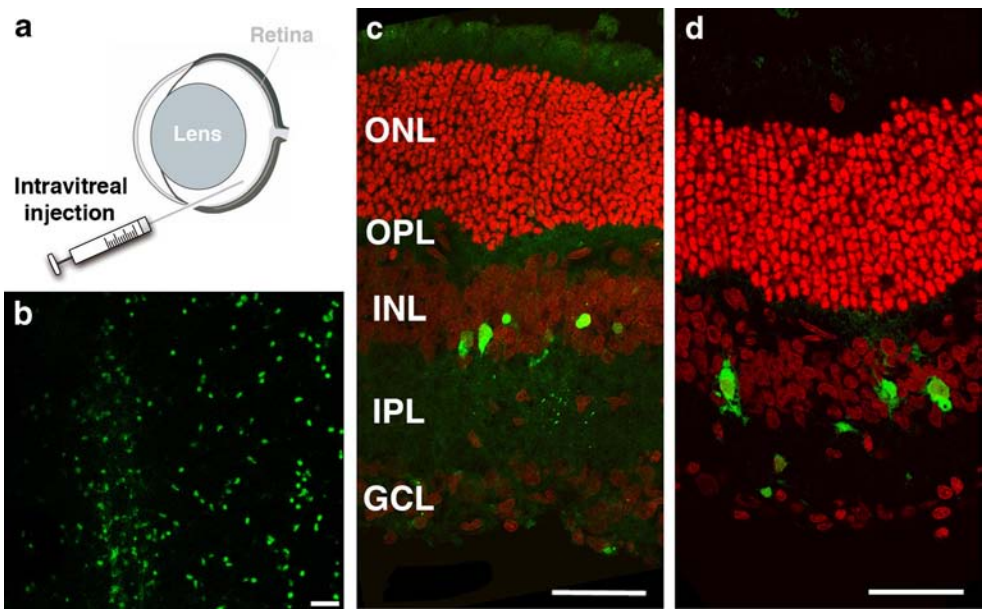

Fig. 6 *In vivo* gene expression of EGFP after administration of lipoplexes at 2/1 ratio to rats 72 h post intravitreal injection. (**a**) Schematic drawing of the intravitreal injection. (**b**) Wholemount view of a transfected retina focused at the inner nuclear layer. Note the mosaic of EGFP expression (*green* labelling). (**c**) Cellular EGFP expression (*green* labelling) is detected in the INL and scarcely in the GCL. (**d**) Cellular EGFP expression (*green* labelling) is also detected in some Müller cells at the INL and scarcely in the GCL. Cell nuclei were counterstaining with Hoechst 33342 (pseudocolored *red*). ONL (Outer nuclear layer), OPL (Outer plexiform layer), INL (Inner nuclear layer), IPL (Inner plexiform layer), GCL (Ganglion cell layer). Scale bars = 40 μm.

We elaborated a novel non-viral formulation based on the combination of the cationic lipid, 2,3-di(tetradecyloxy)propan-1-amine, with the non ionic surfactant polysorbate 80, to deliver the pCMS-EGFP plasmid into rat retinal cells by subretinal and intravitreal injections.

The basic structure of cationic lipids influences on both transfection efficiency and toxicity (22); therefore, it is important to understand the effects of the domains of cationic lipids on the different stages that regulate the transfection processes.

As most of the cationic lipids employed for gene delivery, the 2,3-di(tetradecyloxy)propan-1-amine cationic lipid contains four functional domains: a hydrophilic headgroup, a hydrophobic domain, a linker, and a backbone domain (Supplementary Material). The polar headgroup is an amine positively charged at physiological pH, which allows electrostatic interaction with the DNA. Single amine headgroups are among the most frequently used in many of the established cationic lipids for gene therapy purposes such as DOTMA or DOTAP (23). The non-polar hydrophobic domain consists on two linear saturated C14 aliphatic chains. The structure of the hydrophobic domain affects to the stability of the formulation, the DNA protection from nucleases, the endosomal escape or the nuclear penetration. C14 chain length is optimal for transfection (24). The linker, which governs the relative orientation of the polar head group and the biodegradability, consists on an ether bond, which generally renders good transfection efficiencies; however, ether bonds are too stable to be biodegraded, which results in higher toxicity compounds compared to esters (25). The backbone domain that separates the polar headgroup from the hydrophobic domain has an asymmetric glycerol-based backbone domain, which is the most common used for gene therapy purposes (26).

Regarding the chemical structure of the 2,3-di(tetradecyloxy)propan-1-amine cationic lipid, it is expected to offer a high transfection efficiency, but with questionable cytotoxicity. To overcome this problem, we combined the lipid with the non ionic surfactant polysorbate 80, one of the most employed in the pharmaceutical industry. It has been reported that the addition of polysorbate 80 decreases the proportion of the cationic lipid in the formulation, which reduces the risk of toxicity associated to the cationic lipid (27). Furthermore, the presence of polyethylene glycol (PEG) in its structure improves transfection efficiency when combined with liposomes (28). In addition, polysorbate 80 acts as an emulsifier that avoid aggregations of the particles (29). Therefore, polysorbate 80 is an essential component of our formulation, since when it was not present in the formulation, particles aggregated (data not shown).

Adding DNA to the formulation results in lipoplexes which adopt the most favourable structure conformation form a energetic point of view (30). In our experimental conditions, lipoplexes at 2/1 ratio had a spherical morphology (Fig. 1b, c), and the particle size observed under the microscope was similar to that reported by DLS in Fig. 1a (around 200 nm). It has been widely reported that uptake and transfection efficiency of lipoplexes strongly depends on the size of the vectors (31,32). Although there is not a general rule about the optimum particle size of lipoplexes for gene therapy, it is generally accepted that cationic lipid/DNA ratio is a major determinant of the particle size (30,32). We found that size increased gradually with the mass ratio, reaching a maximum of 260 nm at 4/1 ratio (Fig. 1a, bars). This increment in the particle size can be explained by the greater space demanded by the lipid in the formulation; however, as the proportion of the cationic lipid increases, the DNA is more condensed in the formulation, due to the electrostatic interactions, which could explain the particle size reduction at higher ratios (6/1 and 8/1). Therefore, particle size can depend on the delicate balance between the ability of the cationic lipid to precondense the DNA and the greater space demanded by itself. Regarding zeta potential, we observed a clear direct correlation with the cationic lipid/DNA mass ratio since first zeta potential positive value was obtained at 2/1 ratio (7.3 mV, Fig. 1a, lines), and thereafter increased until a maximum of 13.2 mV at 6/1 ratio. The lower DNA condensation degree at low ratios could explain the low zeta potential values, whereas at high cationic lipid/DNA ratios, the free amine groups of the lipid not neutralised by the negative charges of the plasmid could explain the more positive values observed. Slight reductions of zeta potential values observed at higher ratios (8/1) could be due to limitations associated to the technique. Generally, a net positive charge of the lipoplexes is a desirable characteristic for gene delivery purposes, since it enhances electrostatic interactions with negatively charged membranes and enhances the endocytosis process.

In order to study the binding efficiency between the cationic lipid and the DNA, we designed an agarose gel electrophoresis assay at different mass ratios (Fig. 2). The 0.5/1 and 1/1 ratios were discharged because the negative zeta potential (Fig. 1a, lines). The rest of the formulations were able to complex the DNA, although the weak SC band observed on lane 4 indicates that at 2/1 mass ratio, a small proportion of DNA was unbound; however, this mass ratio was the only one that completely released all the bound DNA after SDS addition, since no DNA signal was observed in the well (lane 5). In contrast, the other proportions had some difficulties to release the DNA, especially after treatment with the enzyme and thereafter with the SDS tensoactive (lanes 9, 12 and 15), probably because lipoplexes were more positively charged. These results emphasize the important role that the cationic lipid/DNA mass ratio plays on the delicate balance between DNA condensation and release.

The capacity of lipoplexes to transfect *in vitro* was evaluated on HEK-293 cells; one of the most employed models for transfection studies, and on a cell line of the retina that support

the photoreceptors at the back of the retina, such as ARPE-19 cells. Mutations in genes specific to this cells can lead to photoreceptors death (33). Transfection was evaluated qualitatively by fluorescent microscopy (Fig. 3) and further checked by flow cytometry quantitatively (Fig. 4). We discharged the 8/1 ratio for the *in vitro* transfection studies due to the data obtained in the agarose electrophoresis assays (Fig. 2). In our experimental conditions the number of HEK-293 and ARPE-19 cells transfected with the lipoplexes increased proportionally to the ratio; however, the greatest percentages of transfection were achieved with Lipofectamine™ 2000. The number of ARPE-19 cells transfected at all ratios was lower but close to HEK-293, which reveals the suitability of this formulation to be applied into the retina, since it has been reported that ARPE-19 cells are more difficult to be transfected than HEK-293 cells (34). Regarding cell viability (Fig. 4b lines), we observed that lipoplexes-induced toxicity increased in a lipid/DNA ratio manner in ARPE-19 cells. Others authors have found the same relationship between toxicity and cationic lipid/DNA mass ratio (35). According with this study, the addition of DNA to the cationic lipid formulation (lipoplexes) resulted in more toxic compounds than the formulation without the DNA. Cytotoxicity effect was associated to the induction of apoptosis in the treated cells. However, in Hek-293 cells, we did not observe a clear relationship between toxicity and cationic lipid/DNA mass ratio, which suggests that the toxicity of the lipoplexes depends, among other factors, on the cell type (30). Interestingly, Lipofectamine™ 2000 (one of the most common used reagents for transfection purposes) was significantly more toxic to HEK-293 (75% viability) and ARPE-19 (71% viability) cells than the lipoplexes at all ratios tested (Fig. 4b, lines). To further relate the percentage of transfected cells and the level of protein expressed, we also measured the MFI of the transfected cells (Fig. 4b, bars and c histograms), since this parameter is also considered for the development of gene therapy vectors (36). Surprisingly, the highest values of MFI in ARPE-19 cells were obtained at low mass ratios 2/1 and 4/1, and were clearly superior to Lipofectamine™ 2000. At high cationic lipid/DNA mass ratio 6/1, MFI clearly decreased, which could be explained by the difficulties of the DNA to be released from the formulation as observed in gel retardation studies (Fig. 2, lane 11). Therefore, and based on the low toxicity, the reasonable percentage of cell transfected and the high MFI values, we carried out a further preliminary *in vivo* study to asses whether the vectors at 2/1 and 4/1 ratios were able to transfect efficiently retinal cells after subretinal (Fig. 5) and intravitreal (Fig. 6) injections.

Subretinal injection resulted in substantial transfection mainly observed in the RPE layer, photoreceptor outer segments (Fig. 6b) and ONL (Fig. 6c). Transfection at this level of the retina is of great interest, since the majority of inherited retinal diseases that cause vision loss worldwide, such as retinitis pigmentosa or age-related macular degeneration, are associated to mutations in genes expressed in the photoreceptor of RPE layer (37,38). However, possible complications related with this route often dissuade its clinical application. By contrast, intravitreal injection is a widely used technique in ophthalmology. Our results shows that intravitreal injections of lipoplexes induced a uniform transfection in a broad surface of the ganglion cell layer (Fig. 6b), which suggests that lipoplexes did not aggregate with the negatively charged components of the vitreous such as glycosamineglycans and diffused to the inner surfaces of the retina, probably due to the ability of the PEG chains of the polysorbate 80 structure to prevent aggregations with fibrilar structures in the vitreous (39). Transfection at the inner layers of the retina could be interesting to treat some genetic pathologies of the retina such us glaucoma (40), a progressive optic neuropathy that affect to retinal ganglion cells.

CONCLUSIONS

In this study we have elaborated and characterized a safe and easy to prepare non-viral vector formulation based on the cationic lipid 2,3-di(tetradecyloxy)propan-1-amine, in combination with the non ionic surfactant polysorbate 80, to transfect efficiently retinal cells. Targeted cells strongly depended on the administration route. Whereas subretinal injections transfected mainly the RPE layer; the intravitreal injection transfected a broad surface in the inner layers of the retina. Although this preliminary study may be useful to select the target cells, additional work would be required to target the outer retina by much safer intravitreal instead of subretinal injections. Likewise, the long term evaluation of the transgene expression should be investigated in order to translate preclinical results in animals to clinical trials.

ACKNOWLEDGMENTS AND DISCLOSURES

This project was partially supported by the University of the Basque Country UPV/EHU (UFI 11/32), by the Research Chair in Retinitis Pigmentosa ¨Bidons Egara¨, and by the National Organization of Spanish Blind People (ONCE). Technical and human support provided by SGIker (UPV/EHU) is gratefully acknowledged.

REFERENCES

1. Lipinski DM, Thake M, Maclaren RE. Clinical applications of retinal gene therapy. Prog Retin Eye Res. 2012;32:22–47.
2. Charbel Issa P, MacLaren RE. Non-viral retinal gene therapy: a review. Clin Experiment Ophthalmol. 2012;40(1):39–47.

3. Liu MM, Tuo J, Chan CC. Gene therapy for ocular diseases. Br J Ophthalmol. 2011;95(5):604–12.
4. Bloquel C, Bourges JL, Touchard E, Berdugo M, BenEzra D, Behar-Cohen F. Non-viral ocular gene therapy: potential ocular therapeutic avenues. Adv Drug Deliv Rev. 2006;58(11):1224–42.
5. Naik R, Mukhopadhyay A, Ganguli M. Gene delivery to the retina: focus on non-viral approaches. Drug Discov Today. 2009;14(5–6): 306–15.
6. Colella P, Auricchio A. Gene therapy of inherited retinopathies: a long and successful road from viral vectors to patients. Hum Gene Ther. 2012;23(8):796–807.
7. Bainbridge JW, Smith AJ, Barker SS, Robbie S, Henderson R, Balaggan K, *et al.* Effect of gene therapy on visual function in leber's congenital amaurosis. N Engl J Med. 2008;358(21):2231–9.
8. Cideciyan AV, Aleman TS, Boye SL, Schwartz SB, Kaushal S, Roman AJ, *et al.* Human gene therapy for rpe65 isomerase deficiency activates the retinoid cycle of vision but with slow rod kinetics. Proc Natl Acad Sci U S A. 2008;105(39):15112–7.
9. Maguire AM, Simonelli F, Pierce EA, Pugh Jr EN, Mingozzi F, Bennicelli J, *et al.* Safety and efficacy of gene transfer for leber's congenital amaurosis. N Engl J Med. 2008;358(21):2240–8.
10. Mussolino C, del la Corte M, Rossi S, Viola F, Di Vicino U, Marrocco E, *et al.* Aav-mediated photoreceptor transduction of the pig cone-enriched retina. Gene Ther. 2011;18(7):637–45.
11. Vandenberghe LH, Bell P, Maguire AM, Cearley CN, Xiao R, Calcedo R, *et al.* Dosage thresholds for aav2 and aav8 photoreceptor gene therapy in monkey. Sci Transl Med. 2011;3(88):88ra54.
12. Bessis N, GarciaCozar FJ, Boissier MC. Immune responses to gene therapy vectors: influence on vector function and effector mechanisms. Gene Ther. 2004;11 Suppl 1:S10–7.
13. Thomas CE, Ehrhardt A, Kay MA. Progress and problems with the use of viral vectors for gene therapy. Nat Rev Genet. 2003;4(5):346–58.
14. Tamboli V, Mishra GP, Mitra AK. Polymeric vectors for ocular gene delivery. Ther Deliv; 2(4):523–536.
15. Liu HA, Liu YL, Ma ZZ, Wang JC, Zhang Q. A lipid nanoparticle system improves sirna efficacy in rpe cells and a laser-induced murine cnv model. Invest Ophthalmol Vis Sci. 2011;52(7):4789–94.
16. Shafaa MW, El Shazly LH, El Shazly AH, El Gohary AA, El Hossary GG. Efficacy of topically applied liposome-bound tetracycline in the treatment of dry eye model. Vet Ophthalmol. 2011;14(1):18–25.
17. Kawakami S, Harada A, Sakanaka K, Nishida K, Nakamura J, Sakaeda T, et al. In vivo gene transfection via intravitreal injection of cationic liposome/plasmid DNA complexes in rabbits. Int J Pharm. 2004;278(2):255–62.
18. Koirala A, Conley SM, Naash MI. A review of therapeutic prospects of non-viral gene therapy in the retinal pigment epithelium. Biomaterials. 2013;34(29):7158–67.
19. Grijalvo S, Ocampo SM, Perales JC, Eritja R. Synthesis of lipid-oligonucleotide conjugates for rna interference studies. Chem Biodivers. 2011;8(2):287–99.
20. Kokotos G, Verger R, Chiou A. Synthesis of 2-oxo amide triacylglycerol analogues and study of their inhibition effect on pancreatic and gastric lipases. Chemistry. 2000;6(22):4211–7.
21. Flannery JG, Visel M. Adeno-associated viral vectors for gene therapy of inherited retinal degenerations. Methods Mol Biol. 2013;935: 351–69.
22. Lv H, Zhang S, Wang B, Cui S, Yan J. Toxicity of cationic lipids and cationic polymers in gene delivery. J Control Release. 2006;114(1): 100–9.
23. Morille M, Passirani C, Vonarbourg A, Clavreul A, Benoit JP. Progress in developing cationic vectors for non-viral systemic gene therapy against cancer. Biomaterials. 2008;29(24–25):3477–96.
24. Lenssen K, Jantscheff P, von Kiedrowski G, Massing U. Combinatorial synthesis of new cationic lipids and high-throughput screening of their transfection properties. Chembiochem. 2002;3(9): 852–8.
25. Aberle AM, Tablin F, Zhu J, Walker NJ, Gruenert DC, Nantz MH. A novel tetraester construct that reduces cationic lipid-associated cytotoxicity. Implications for the onset of cytotoxicity. Biochemistry. 1998;37(18):6533–40.
26. Zhi D, Zhang S, Wang B, Zhao Y, Yang B, Yu S. Transfection efficiency of cationic lipids with different hydrophobic domains in gene delivery. Bioconjug Chem. 2010;21(4):563–77.
27. del Pozo-Rodriguez A, Delgado D, Solinis MA, Gascon AR, Pedraz JL. Solid lipid nanoparticles: formulation factors affecting cell transfection capacity. Int J Pharm. 2007;339(1–2):261–8.
28. Meyer O, Kirpotin D, Hong K, Sternberg B, Park JW, Woodle MC, *et al.* Cationic liposomes coated with polyethylene glycol as carriers for oligonucleotides. J Biol Chem. 1998;273(25):15621–7.
29. Liu F, Yang J, Huang L, Liu D. Effect of non-ionic surfactants on the formation of DNA/emulsion complexes and emulsion-mediated gene transfer. Pharm Res. 1996;13(11):1642–6.
30. Ma B, Zhang S, Jiang H, Zhao B, Lv H. Lipoplex morphologies and their influences on transfection efficiency in gene delivery. J Control Release. 2007;123(3):184–94.
31. Conner SD, Schmid SL. Regulated portals of entry into the cell. Nature. 2003;422(6927):37–44.
32. Ross PC, Hui SW. Lipoplex size is a major determinant of in vitro lipofection efficiency. Gene Ther. 1999;6(4):651–9.
33. McClements ME, MacLaren RE. Gene therapy for retinal disease. Transl Res. 2013;161(4):241–54.
34. del Pozo-Rodriguez A, Delgado D, Solinis MA, Gascon AR, Pedraz JL. Solid lipid nanoparticles for retinal gene therapy: transfection and intracellular trafficking in rpe cells. Int J Pharm. 2008;360(1–2):177–83.
35. Nguyen LT, Atobe K, Barichello JM, Ishida T, Kiwada H. Complex formation with plasmid DNA increases the cytotoxicity of cationic liposomes. Biol Pharm Bull. 2007;30(4):751–7.
36. Villa-Diaz LG, Garcia-Perez JL, Krebsbach PH. Enhanced transfection efficiency of human embryonic stem cells by the incorporation of DNA liposomes in extracellular matrix. Stem Cells Dev. 2010;19(12): 1949–57.
37. Hims MM, Diager SP, Inglehearn CF. Retinitis pigmentosa: genes, proteins and prospects. Dev Ophthalmol. 2003;37:109–25.
38. Conley SM, Naash MI. Nanoparticles for retinal gene therapy. Prog Retin Eye Res. 2010;29(5):376–97.
39. Peeters L, Sanders NN, Braeckmans K, Boussery K, Van de Voorde J, De Smedt SC, *et al.* Vitreous: a barrier to nonviral ocular gene therapy. Invest Ophthalmol Vis Sci. 2005;46(10):3553–61.
40. Liu X, Rasmussen CA, Gabelt BT, Brandt CR, Kaufman PL. Gene therapy targeting glaucoma: where are we? Surv Ophthalmol. 2009;54(4):472–86.